Energy modulation of nonrelativistic electrons in an optical near field on a metal microslit

R. Ishikawa,[a] J. Bae, and K. Mizuno
Research Institute of Electrical Communication, Tohoku University, 2-1-1 Katahira, Aoba-ku, Sendai 980-8577, Japan

(Received 15 September 2000; accepted for publication 4 December 2000)

Energy modulation of nonrelativistic electrons with a laser beam using a metal microslit as an interaction circuit has been investigated. An optical near field is induced in the proximity of the microslit by illumination of the laser beam. The electrons passing close to the slit are accelerated or decelerated by an evanescent wave contained in the near field whose phase velocity is equal to the velocity of the electrons. The electron–evanescent wave interaction in the microslit has been analyzed theoretically and experimentally. The theory has predicted that electron energy can be modulated at optical frequencies. Experiments performed in the infrared region have verified theoretical predictions. The electron–energy changes of more than ± 5 eV with a 10 kW CO_2 laser pulse at the wavelength of 10.6 μm has been successfully observed for an electron beam with an energy of less than 80 keV. © *2001 American Institute of Physics.* [DOI: 10.1063/1.1345851]

I. INTRODUCTION

Electron beam devices have several advantages over solid state devices, such as wider tuning frequency range and higher output power. Those devices using nonrelativistic electrons, klystrons, and traveling wave tubes, are mostly for microwave region.[1] Only free electron lasers can operate at optical frequencies, but these utilize relativistic electron beams for laser action and consequently their device size is huge.[2] To develop compact convenient beam devices, the use of nonrelativistic electrons is indispensable. However, there are few reports on the theoretical and experimental studies for the interaction between lower energy electrons and light. Schwarz and Hora reported that a 50 keV electron beam passing through a thin dielectric film was modulated with an argon laser beam at the wavelength of 488 nm.[3] This effect, however, has not yet been reproduced by other experimental groups. Successful experiments on the (inverse) Smith–Purcell effect[4] using nonrelativistic electron beams have been reported, but the operation frequencies still remain in the far-infrared region.[5,6]

In order to realize significant coupling between visible or infrared waves and a nonrelativistic electron beam, a metal microslit has been proposed.[7] In Fig. 1, an optical near field is induced in the proximity of the microslit with laser illumination. Energy of electrons passing close to the surface of the slit is modulated with a laser. This type of metal microslit is more suitable than the dielectric film for precise measurement of energy exchange between free electron and light and for investigating quantum effects[8,9] that will be happened in the interaction, because there is not a disturbance such as electron scattering in dielectric medium.

Using the metal microslit, we have demonstrated the energy modulation of an electron beam with a CO_2 laser at the wavelength of 10.6 μm.[10] The experimental results have verified theoretical predictions for relationship among laser wavelength, initial electron velocity, and slit width. In this article, the theoretical and the experimental results for the microslit interaction circuit are presented.

II. THEORY

A. Near-field distributions

According to Chou and Adams's analysis,[11] near-field distributions on a metal microslit have been calculated using the method of moments. For ease of the calculation, it has been assumed that (1) the metal slit consists of two semi-infinite plane screens with a perfect conductance and a zero thickness, and (2) a normally incident plane wave is polarized perpendicularly to the slit.

In order to verify the theory, near-field intensity distributions on a metal slit have been measured using a scaled model of the slit at a microwave frequency of 9 GHz (wavelength $\lambda = 33$ mm). The experimental setup is shown in Fig. 2. The metal slit consists of two aluminum plates with a height of 400 mm, a width of 190 mm, and a thickness of 1 mm. The rectangular horn antenna with an aperture size of 116 mm$\times$157 mm was placed at the distance of 1650 mm from the slit. This longer distance assures a plane wave incidence. The small antenna probe detects an electric field in the x direction $|E_x|$ which is a dominant field for the interaction with electrons.

The antenna probe with a length of 1.6 mm was placed at the end of a thin coaxial cable with a diameter of 0.8 mm connected to a spectrum analyzer HP-8562B. In order to avoid an influence of a reflected wave from the slit upon the near-field distributions, the probe was placed at the opposite side of the horn.

Figure 3 compares the calculated [3(a)] and measured [3(b)] field intensity distributions of $|E_x|$ on the slit. The slit width d was 0.5 λ. The field intensities were normalized to the one $|E_{xi}|$ measured at $x=y=0$ without the slit. In Fig. 3,

[a]Electronic mail: issi@riec.tohoku.ac.jp

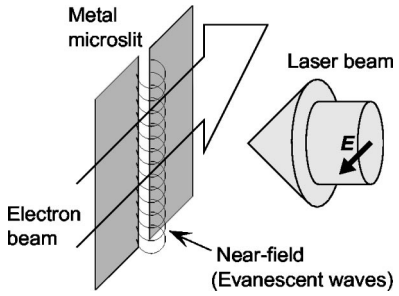

FIG. 1. Conceptual drawing of electron-light energy exchanges using a metal microslit.

the shapes of the field distributions for both the theory and the experiment are quite similar, though the measured near field in Fig. 3(b) has small ripples. These result from the interference of waves scattered from the coaxial probe and the slit.

Figure 4 shows the calculated and measured field intensities for the slits with different widths as a function of the distance from the slit surface y at the center of the slit, i.e., $x=0$. In the results for $d=0.75\lambda$, the theory has agreed well with the measurement. When d decreases 0.75 λ to 0.12 λ, deviations of the measured intensities from the theoretical ones increase mainly due to the probe having a finite size of about 0.05 λ. However, the theory has well predicted the measured variations of the field intensities with y. Those results indicate that the theory is valid allowing for experimental errors.

B. Electron-energy changes

Using the theoretical near-field distributions, energy changes of electrons passing close to the slit surface were estimated through computer simulation.[12] The theoretical model used for the calculation is shown in Fig. 5. The electrons with a velocity v_i move in the x direction at the distance y_i from the surface of the slit. All field components, i.e., electric fields E_x, E_y, and a magnetic field H_z in the near field were taken into account for calculation. The total energy changes of the electrons were determined by integrating small energy changes with the Lorentz force in a small distance along the electron trajectory. The integral length L was chosen to be ten times of the slit width which fully covers the near-field region on the slit.

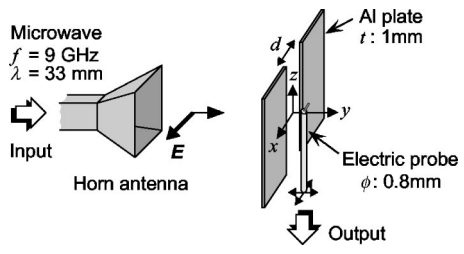

FIG. 2. Experimental setup for measurement of near-field distributions on a metal slit at 9 GHz. A small electric probe detects an electric field in the x direction $|E_x|$. The field distributions in the proximity of the slit were measured by scanning the probe in the x and y directions.

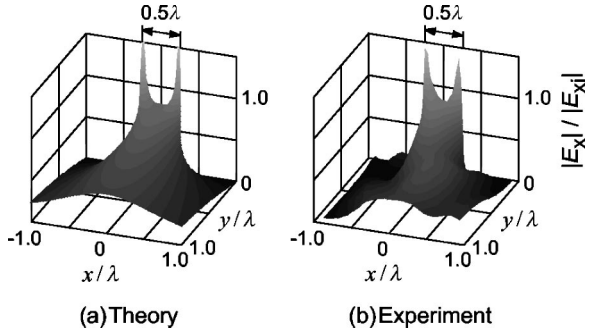

FIG. 3. (a) Calculated and (b) measured field intensity distribution of $|E_x|$ on a slit with a width of 0.5 λ. The field intensities were normalized to the field $|E_{xi}|$ measured at $x=y=0$ without the slit.

Figure 6 shows the calculated maximum energy changes ΔW for the electrons with different velocities β $(=v_i/c$, c: light speed) as a function of d at $y_i=0.01\lambda$. ΔW is normalized to the maximum value in the curve for $\beta=0.5$ at $d/\lambda=0.64$. As seen from Fig. 6, the curve for $\beta=0.3$ has two peaks of 0.63 and 0.68 at $d=0.08\,\lambda$ and 0.38 λ, respectively. These slit widths correspond to the transit angles, θ $(=\omega d/v_i)=0.53\pi$ and $2.53\ \pi$ for the electrons, where ω is the angular frequency of the laser. As β increases, the optimum slit widths d_m become wider to keep the transit angle same. From those calculation results, the following relationship between d_m and β was found:

$$d_m \cong \beta\lambda(m+\tfrac{1}{4}), \tag{1}$$

where m is an integer. It should be noted that the optimum width is narrower than that in a conventional metal parallel plate circuit as used in klystrons.[7] In this circuit, electrons are modulated with a uniform field at the gap between the parallel plates. It is known that the optimum gap width is given by $\beta\lambda(m+1/2)$. The difference of $\beta\lambda/4$ between the optimum widths would arise from the difference of the field distributions in the two circuits.

In Fig. 6, the second peaks in the ΔW curves at the wider width are always larger than the first peaks at the narrower width. In the slit circuit, ΔW is roughly proportional to

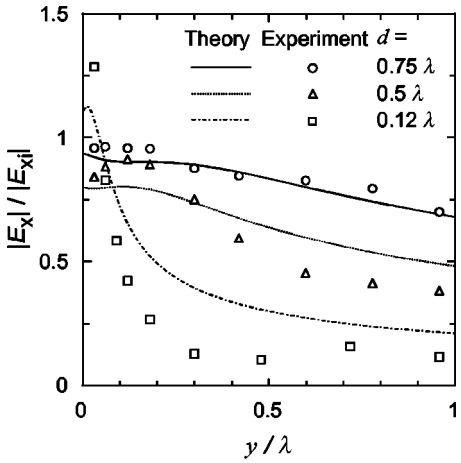

FIG. 4. Comparison between the calculated and measured field intensities for the slits with widths of 0.75 λ, 0.5 λ, and 0.12 λ, as a function of the distance from the slit surface y at $x=0$.

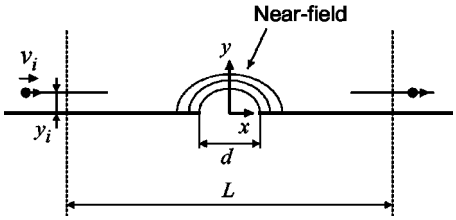

FIG. 5. Calculation model of electron energy changes with a near field on a slit of a width d. An electron, with an initial velocity v_i and its position y_i, is accelerated or decelerated by Lorentz force in the near-field region. The integration length L of ten times the slit width was chosen to fully cover the near-field region on the slit.

the field intensity E_x and an effective interaction length in the slit. As seen from Fig. 4, E_x for the wider slit width is smaller than or nearly equal to the one for the narrower width at $y=0.01\,\lambda$. The increase of the interaction length thus exceeds the decrease of the field intensity when the slit width increases.

Figure 7 shows the calculated ΔW for different electron velocities as a function of the position y. Slits having the optimum slit widths of $d_m/\lambda=(0.38,\ 0.5,\ \text{and}\ 0.62)$ for $\beta=(0.3,\ 0.4,\ \text{and}\ 0.5)$, respectively, were used for calculation. A CO_2 laser beam with $\lambda=10.6\,\mu$m and a power density of 3×10^7 W/cm^2 was assumed as the incident wave. This power density corresponds to a 10 kW output power focused onto a 200 μm diameter area.

In Fig. 7, when y increases from zero to 0.5 λ, ΔW falls off exponentially to near zero. The decay constants for the exponential curves were estimated to be $\alpha_0=k_0\times(3.2,\ 2.3,\ \text{and}\ 1.7)$ for $\beta=(0.3,\ 0.4,\ \text{and}\ 0.5)$, respectively, where k_0 is the wave number of the laser beam in free space. Since ΔW is proportional to a field intensity, those curves represent effective field distributions for the electrons in the slit.

The effective field distributions shown in Fig. 7 are considerably different from the near-field distributions in Fig. 4. The near fields on the slit contain a number of wave components with different wave numbers k_x in the x-direction in

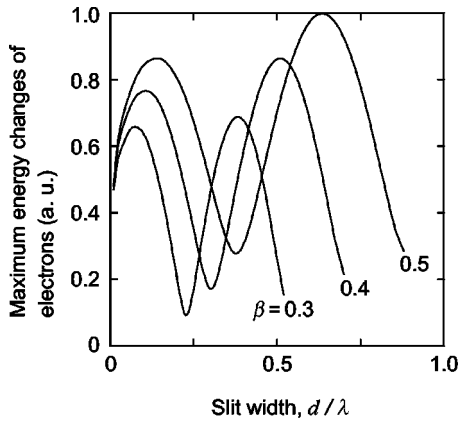

FIG. 6. Calculated maximum energy changes of electrons as a function of the slit width d for different electron velocities $\beta=v_i/c$ of 0.3, 0.4, and 0.5 at $y=0.01\,\lambda$. The energy changes are normalized to the maximum one in the curve for $\beta=0.5$ at $d=0.62\,\lambda$. The slit width is also normalized to the wavelength.

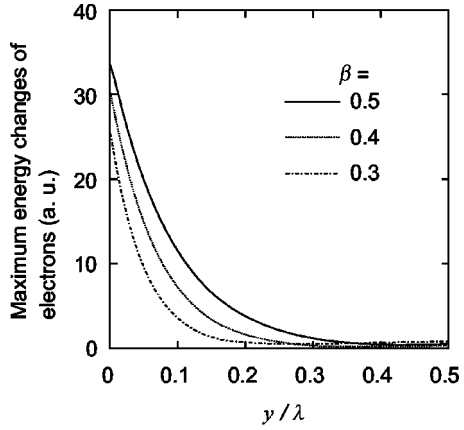

FIG. 7. Calculated maximum energy changes of electrons as a function of y/λ for different electron velocities $\beta=0.3$, 0.4, and 0.5.

Fig. 5. When k_x is larger than k_0, the wave component is an evanescent wave whose field intensities in the slit decays exponentially as y increases. Therefore, it can be deduced that the exponential decay of ΔW in Fig. 7 results from the interaction with the evanescent wave. The decay constant α of the evanescent wave is given by[13,14]

$$\alpha=k_0\sqrt{\left(\frac{k_x}{k_0}\right)^2-1}. \tag{2}$$

Comparing α_0 with α, the following relationship has been found:

$$k_x=\omega/v_i. \tag{3}$$

Therefore, the calculated results indicate that in the slit circuit, electrons with a velocity v_i interact selectively with the evanescent wave whose phase velocity $v_p=\omega/k_x$ is equal to v_i. An effective interaction space of the slit can be defined as $y_e=1/\alpha$, because the field intensity of the evanescent wave falls off by e^{-1}. Using Eqs. (2) and (3), y_e is expressed as

$$y_e=\frac{\lambda}{2\pi}\frac{\beta}{\sqrt{1-\beta^2}}. \tag{4}$$

Equation (4) indicates that the interaction space in the slit circuit is strongly limited, particularly for a lower-energy electron beam. The electrons thus must be passed very close to the slit surface to obtain significant energy exchanges with a laser beam. This is the main reason why we have chosen an infrared laser with a longer wavelength for the first experiment. From the ΔW curve for $\beta=0.5$ in Fig. 7, it is seen that the interaction space is about 3 μm, where measurable electron-energy changes of greater than 1 eV are obtained.

III. EXPERIMENTS

Experiments have been done to verify the theory in the infrared region. The experimental setup is shown in Fig. 8. An electromechanical Q-switched CO_2 laser[15] has been developed and used for the experiments. This laser oscillates in the fundamental transverse electromagnetic (TEM_{00}) mode and generates the output pulses with the maximum peak

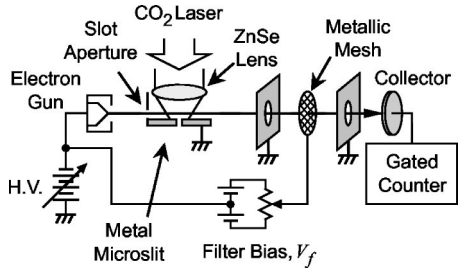

FIG. 8. Experimental setup.

power of 10 kW, a width of 120 ns, and a repetition rate of 1 kpps at $\lambda = 10.6\,\mu$m. The laser beam was focused onto the slit surface with a diameter of about 200 μm using a ZnSe lens. The slit consists of two polished copper blocks, and the width is 8.4 μm. The initial energy W_i of the electron beam was adjusted between 40 and 90 keV. The slot aperture placed in front of the slit confines the beam area on the slit to 10 μm in height and 100 μm in width. The electron energy was measured by using a retarding field analyzer.[16] This analyzer passes all the higher-energy electrons than the filter bias V_f which is a variable retarding potential.

The pulsed laser output modulates the energy of the electron beam, so that the electron current through the analyzer changes during the pulse. The electrons passed through the energy analyzer were detected by a secondary electron multiplier (collector) connected to a gated counter which is triggered by the laser pulse.

Figure 9(a) shows the measured energy spectra of the electrons A with and B without laser illumination, while 9(b) shows the difference between the two spectra A–B. The peak power of the laser was 10 kW and $W_i = 80$ keV. The ordinates are the output counts from the gated counter with a

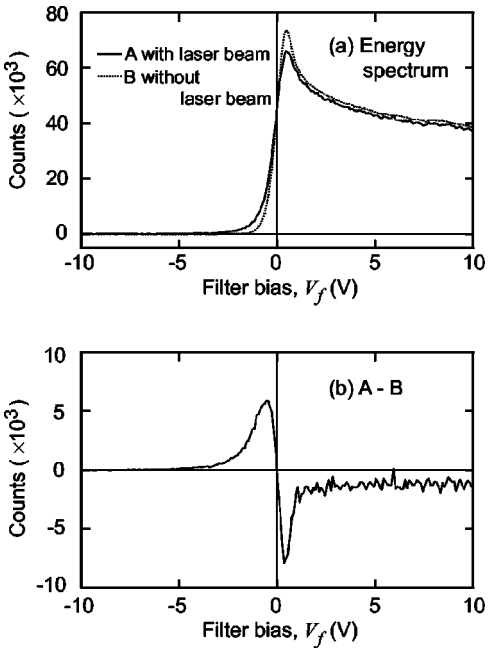

FIG. 9. (a) Measured electron-energy spectra A with and B without laser illumination, and (b) the difference between the two spectra A–B for an electron beam with an initial energy of 80 keV.

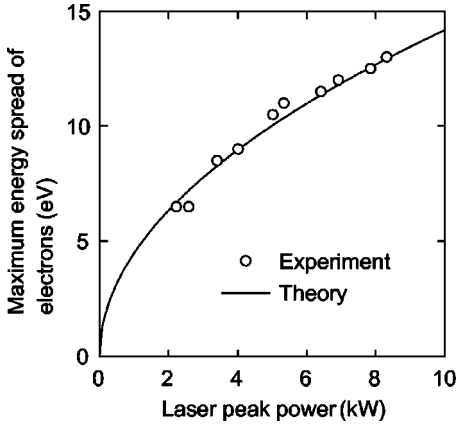

FIG. 10. Maximum energy spread of the electrons as a function of the laser peak power. The solid curve is a theoretical fit to the measurements.

gate width of 1.5 μs and an integration time of 10 s. In this experiment, the electron current was limited to be less than 2 pA to maintain linear response of the electron multiplier even for the larger current input at $V_f > 0$.

In Fig. 9(a), the measured spectrum B without laser illumination shows that our energy analyzer has a resolution better than 0.8 eV for the 80 keV electron beam. The output count decreases gradually as V_f increases from +1 eV due to the dispersion of the energy analyzer. When the laser beam irradiates the electrons, the spectrum B is changed to the spectrum A with a wider energy spread. The spectrum A still contains a number of electrons that have not interacted with the light. In order to remove these electrons and the dispersion effect from the measured spectrum A, the output counts in B were subtracted from those in A. Figure 9(b) thus indicates the energy spectrum only for the electrons that were interacted with the light. From Fig. 9(b), it is seen that the 10 kW laser beam can give the energy spread of more than ± 5 eV to the electrons. The experimental results clearly show that using the metal slit, the energy of the electrons can be modulated with the laser at $\lambda = 10.6\,\mu$m.

Since the energy analyzer passes all the higher-energy electrons, it is expected that, for large bias voltages the output counts with laser illumination should be same as the ones without laser illumination. However as shown in Fig. 9(b), the counts with laser illumination is slightly smaller than the one without laser illumination even at $V_f > +10$ V. This would be due to deflection of the electron beam with the laser illumination. Consequently, a part of the electron beam has been clipped by the aperture before the collector.

In Figs. 9(a) and (b), about 70 000 electrons have passed on the slit, and about 13 000 electrons among them have interacted with the laser beam. Since the height of the electron beam on the slit is 10 μm, this ratio of the signal electrons to the total ones implies that the interaction space of the slit is about 2 μm which agrees with the theoretical prediction as described earlier.

A variation of the maximum energy spread of electrons with the incident laser power has been measured and plotted in Fig. 10. In the experiment, the energy spreads were measured for the electrons with $W_i = 80$ keV and a current of 0.5 nA at $V_f < -3$ eV. The solid curve indicates the theoretical

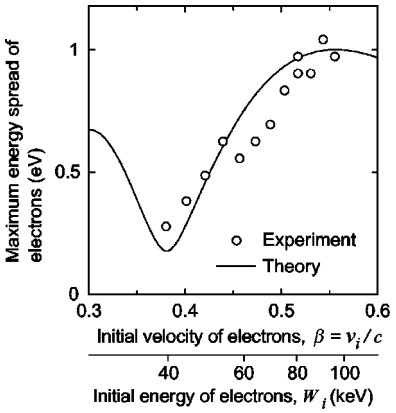

FIG. 11. Maximum energy spread of the electrons as a function of the initial electron velocity. The solid curve indicates the theoretical changes of the electron energy in the slit with a width of 7.2 μm.

variation of the electron energy which is proportional to the field intensity of the incident wave, i.e., the square root of the laser power. The theory has agreed well with the measurements. The measured electron-energy spread is 13 eV at the laser power of 8.3 kW which is compared to the theoretical value of 22 eV predicted through the computer simulation. The reduction of the energy spread would arise from differences of the actual slit from the theoretical slit. Since the actual slit has consisted of the two thick copper blocks with finite conductance, the amplitude of the evanescent wave may be small compared to the theoretical one.

Figure 11 shows the measured electron energy spreads as a function of W_i. In Fig. 11, the electron velocity corresponding to W_i is also indicated. The solid curve is the theoretical variation of the electron energy fitted to the measured ones by adjusting the slit width d. The best fit was obtained for $d=7.2\,\mu$m. The measured and theoretical energy spreads of the electrons have been normalized to the maximum values, 15 eV for the measurement and 34 eV for the theory, respectively, at $W_i=90$ keV. Those experimental results have verified the theory for the metal microslit circuit allowing for experimental errors. In Fig. 11, the electron-energy spread is 4 eV at $W_i=40$ keV. The small modulation at the low W_i could be increased by adjusting the slit width. The results indicate that the metal microslit can be used to modulate a nonrelativistic electron beam at the optical frequency.

IV. CONCLUSIONS

Energy changes of nonrelativistic electrons in an infrared near-field region on a metal microslit have been analyzed theoretically and experimentally. The theoretical analyses have revealed that an evanescent wave contained in the near field interacts with the electrons when the phase velocity of the wave is equal to the velocity of the electrons, this is, the synchronous condition is achieved. Using the metal microslit with a width of about 8.4 μm, the energy modulation of electrons with a CO_2 laser at the wavelength of 10.6 μm has been successfully observed for electron beams with initial energy between 40 and 90 keV. The results could be useful for developing an infrared region grating linac (inverse Smith–Purcell type laser accelerator).[17] In addition, the theoretical and experimental results also imply that developing of a new type of scanning optical near-field microscopes utilizing an electron beam as a near-field probe would be possible.[18]

ACKNOWLEDGMENTS

The authors would like to acknowledge Professor M. Yokoo at Tohoku University, Professor M. Ohtus at Tokyo Institute of Technology, and Professor H. Hori at Yamanashi University for helpful discussions. They are also grateful to K. Sugawara, R. Yonezawa, and K. Takahashi for fabricating the experimental apparatus. This work was partially supported by a Grant in Aid for Scientific Research on Priority Areas from the Ministry of Education, Science, Sports and Culture, Japan.

[1] R. G. E. Hutter, in *Beam and Wave Electronics in Microwave Tubes*, edited by H. J. Reich (Van Nostrand, Toronto, 1960).
[2] C. A. Brau, in *Free-Electron Lasers*, edited by P. W. Hawkes (Academic, San Diego, 1990).
[3] H. Schwarz and H. Hora, Appl. Phys. Lett. **15**, 349 (1969).
[4] S. J. Smith and E. M. Purcell, Phys. Rev. **92**, 1069 (1953).
[5] K. Mizuno, J. Bae, T. Nozokido, and K. Furuya, Nature (London) **328**, 45 (1987).
[6] J. Bae, H. Shirai, T. Nishida, T. Nozokido, K. Furuya, and K. Mizuno, Appl. Phys. Lett. **61**, 870 (1992).
[7] J. Bae, S. Okuyama, T. Akizuki, and K. Mizuno, Nucl. Instrum. Methods **331**, 509 (1993).
[8] K. Mizuno and S. Ono, Proc. IEEE **63**, 1075 (1975).
[9] I. R. Senitzky, Phys. Rev. **95**, 904 (1954).
[10] J. Bae, R. Ishikawa, S. Okuyama, T. Miyajima, T. Akizuki, T. Okamoto, and K. Mizuno, Appl. Phys. Lett. **76**, 2292 (2000).
[11] T. Y. Chou and A. T. Adams, IEEE Trans. Electromagn. Compat. **19**, 65 (1997).
[12] R. Ishikawa, J. Bae, and K. Mizuno, *Technical Digest of the 5th International Conference on Near Field Optics* (Shirahama, 1998), p. 173.
[13] G. A. Massey, Appl. Opt. **23**, 658 (1984).
[14] D. P. Tsai, H. E. Jackson, R. C. Reddick, S. H. Sharp, and R. J. Warmack, Appl. Phys. Lett. **56**, 1515 (1990).
[15] J. Bae, T. Nozokido, H. Shirai, H. Kondo, and K. Mizuno, IEEE J. Quantum Electron. **30**, 887 (1994).
[16] J. F. Graczyk and S. C. Moss, Rev. Sci. Instrum. **40**, 424 (1969).
[17] K. Mizuno, S. Ono, and O. Shimoe, Nature (London) **253**, 184 (1975).
[18] J. Bae, T. Nozokido, T. Okamoto, T. Fujii, and K. Mizuno, Appl. Phys. Lett. **71**, 3581 (1997).